

SAND 95-3060 C  
CONF-951155--29

**SURFACE MORPHOLOGY AND MICROSTRUCTURE OF Al-O ALLOYS  
GROWN BY ECR PLASMA DEPOSITION**

D.A. MARSHALL\*, J.C. BARBOUR\*\*, D.M. FOLLSTAEDT\*\*, A.J. HOWARD\*\*, and  
R.J. LAD\*

\*Laboratory for Surface Science and Technology, University of Maine, Orono, ME 04469

\*\*Sandia National Laboratories, Albuquerque, NM 87185-1056

### ABSTRACT

The growth of polycrystalline and amorphous aluminum-oxygen alloy films using electron-beam evaporation of Al in the presence of an O<sub>2</sub> electron-cyclotron-resonance (ECR) plasma was investigated for film compositions varying from 40% Al (Al<sub>2</sub>O<sub>3</sub>) to near 100% Al (AlO<sub>x</sub>). Processing parameters such as deposition temperature and ion energy were varied to study their effects on surface texture and film microstructure. The Al-rich films (AlO<sub>x</sub>) contain polycrystalline fcc Al grains with finely dispersed second-phase particles of  $\gamma$ -Al<sub>2</sub>O<sub>3</sub> (1-2 nm in size). The surface roughness of these films was measured by atomic force microscopy and found to increase with sample bias and deposition temperature. Stoichiometric Al<sub>2</sub>O<sub>3</sub> films grown at 100°C and 400°C without an applied bias were amorphous, while an applied bias of -140 V formed a nanocrystalline  $\gamma$ -Al<sub>2</sub>O<sub>3</sub> film at 400°C. The surface roughness of the Al<sub>2</sub>O<sub>3</sub> increased with temperature while ion irradiation produced a smoother surface.

### INTRODUCTION

Aluminum alloys are used in industrial applications requiring high strength and light weight, but poor tribological properties for some of these alloys can limit their use. In these cases, the deposition of hard, wear resistant coatings can extend the use of Al alloys, such as with coatings on turbine blades. High strength has recently been achieved for aluminum-oxygen alloy films of varying stoichiometries and microstructure ranging from hard, dispersion-strengthened AlO<sub>x</sub> layers [1-5] to Al<sub>2</sub>O<sub>3</sub> layers that are also expected to be hard and wear resistant. Dispersion-strengthened AlO<sub>x</sub> films consist of a fcc Al matrix containing finely dispersed  $\gamma$ -Al<sub>2</sub>O<sub>3</sub> precipitates which strengthen the film by blocking dislocation motion [3, 6]. The critical shear stress for the extrusion of a dislocation through the hard precipitates is given by  $Gb/L$ , where  $G$  is the shear modulus of the Al matrix,  $b$  is the burgers vector, and  $L$  is the inter-particle spacing. As precipitate density increases, the critical shear stress increases and correspondingly the yield stress increases. Ideally, AlO<sub>x</sub>/Al<sub>2</sub>O<sub>3</sub> multilayers can be grown for use as hard coatings which combine the hardness of Al<sub>2</sub>O<sub>3</sub> with the ductility of aluminum. However, control of the surface morphology for these layers is critical for obtaining the desired tribological properties.

Several techniques including ion implantation [1-5], electron-cyclotron-resonance (ECR) plasma growth [6,7], and pulsed laser deposition (PLD) [8] have been used at Sandia National Laboratories to grow AlO<sub>x</sub> hard layers. Ion implantation has been used to demonstrate that AlO<sub>x</sub> films can be produced with yield stresses up to 2.9 GPa as a result of dispersion strengthening. However, the implementation of this synthesis technique can be limited by high costs and the thickness of the implanted layer is often less than 1  $\mu$ m. The ECR and PLD methods for depositing AlO<sub>x</sub> layers offer many attractive qualities for production manufacturing. For example, both techniques are scaleable to thick film deposition over large areas and at low temperatures. Also, the composition of the films can be varied over a large range and can be controlled with depth. For ECR plasma deposition, independent control of deposition parameters

including ion energy, temperature, and plasma density allows accurate control of film composition and microstructure. In this paper, we will examine the effects of ion energy and deposition temperature on the film microstructure and surface roughness for ECR plasma-deposited Al(O) alloys.

## EXPERIMENTAL

AlO<sub>x</sub> and Al<sub>2</sub>O<sub>3</sub> samples were deposited onto Si (100) substrates by electron-beam evaporation of Al in the presence of an O<sub>2</sub> plasma generated by a broad-area ECR source; the source operates at 2.45 GHz microwave frequency with the resonance condition created by two electromagnets generating a 875 G magnetic field. Langmuir probe and optical spectroscopy measurements during ECR operation in the pressure range of 2 to 7 x 10<sup>-5</sup> Torr indicate that the predominant species in the oxygen plasma are O<sub>2</sub><sup>+</sup> ions [6]. The AlO<sub>x</sub> and Al<sub>2</sub>O<sub>3</sub> films were grown by independently varying the following parameters: Al deposition rate (0.2 to 3.0 nm/sec), applied dc bias (0 to -300 V), O<sub>2</sub> flow rate (0.7 to 2.5 sccm), total chamber pressure (2 to 7.5 x 10<sup>-5</sup> Torr), microwave power (35 to 150 W), and substrate temperature (100 to 400°C). Deposited films were characterized using Rutherford Backscattering Spectrometry (RBS) in order to determine the composition and thickness of the films, Transmission Electron Microscopy (TEM) to determine the crystallinity and microstructure, and Atomic Force Microscopy (AFM) for measuring the surface roughness. The films in this study ranged in thickness from 100-900 nm. In addition, samples grown under similar conditions were examined using ultra-low load nanoindentation (NANO Instruments Nano-Indenter II<sup>®</sup>) for the film hardness and elasticity. Nanoindentation measurements were performed on both pure Al and AlO<sub>x</sub> films, for which three sets of measurements were taken at total penetration depths of 50, 100, and 200 nm. The results indicate a large increase in hardness (3.2 GPa) for the AlO<sub>x</sub> film (20 at.% O) grown at 100°C over that for the pure Al film (hardness ~ 0.9 GPa) as a result of the dispersion strengthening [6]. A dramatic decrease in hardness was found [7] for AlO<sub>x</sub> samples grown at higher temperatures (400°C) and therefore the surface morphology and sample microstructure were examined for samples from these two deposition-temperature regimes.

### Al<sub>2</sub>O<sub>3</sub> FILMS

Al<sub>2</sub>O<sub>3</sub> films were deposited onto Si (100) substrates without an applied bias and with an applied bias up to -155 V, over the temperature range from 100 to 400°C. RBS indicated that all of these films nominally had a stoichiometric Al<sub>2</sub>O<sub>3</sub> composition. TEM results shown in Fig. 1c reveal that the sample grown at 400°C with a -140 V bias is polycrystalline  $\gamma$ -Al<sub>2</sub>O<sub>3</sub> with grains ranging in size from 10 to 40 nm. The use of the substrate bias was crucial in order to obtain a crystalline Al<sub>2</sub>O<sub>3</sub> phase at this relatively low temperature. At 130°C with no bias, an amorphous film was produced as shown in Fig. 1a. Similarly, amorphous films were produced for a deposition temperature of 400 °C without an applied bias, or for deposition temperatures  $\leq$  250°C with a bias of -155 V. The amorphous film shown in Fig. 1a was crystallized *ex-situ* via a post-deposition annealing treatment at 800°C as shown in Fig. 1b, but the grain size is larger than found for the polycrystalline film grown using a biased plasma and 400°C deposition temperature. *In-situ* formation of the crystalline phase occurred only at 400°C in the presence of an applied -140 V bias, which we believe enhanced the mobility of the atoms in the film as a result of irradiation from the energetic plasma ions. Films deposited at lower temperatures with

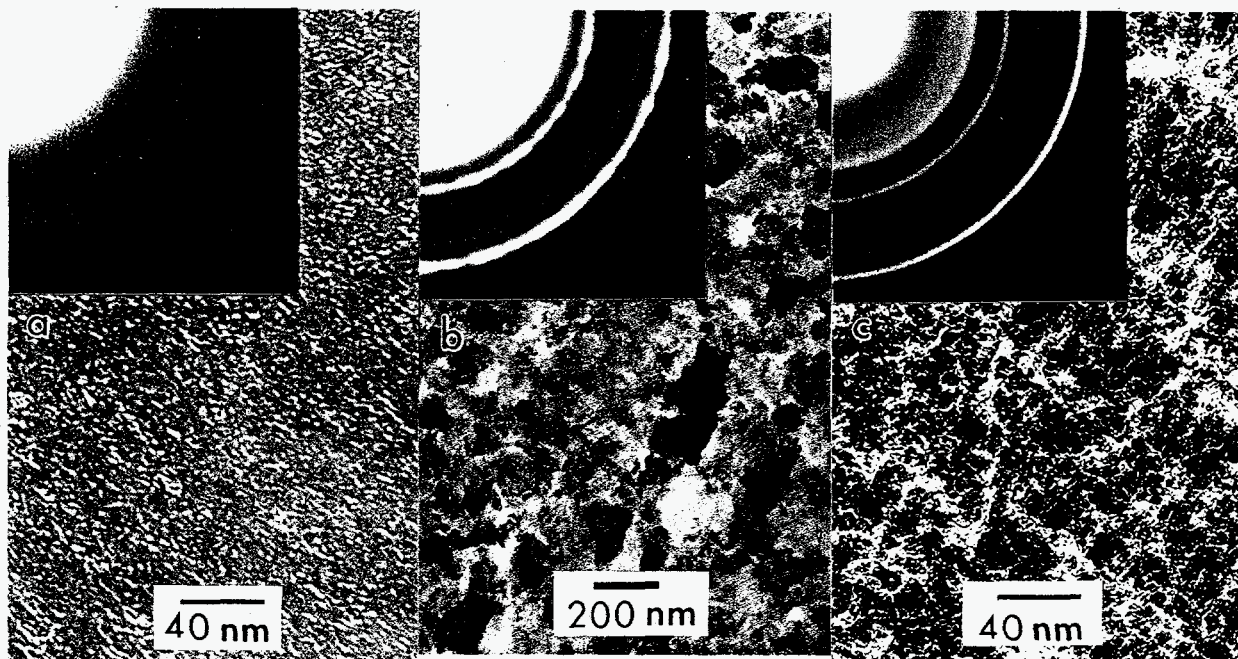


Fig. 1. Bright-field TEM images and diffraction patterns of  $\text{Al}_2\text{O}_3$  films deposited on  $\text{SiO}_x$ -coated TEM grids: (a) amorphous film deposited at  $130^\circ\text{C}$  with no bias, (b) the same film as in (a) which crystallized as  $\gamma\text{-Al}_2\text{O}_3$  after 1.5 hours at  $800^\circ\text{C}$ , and (c) crystalline  $\gamma\text{-Al}_2\text{O}_3$  film deposited at  $400^\circ\text{C}$  with a  $-140\text{ V}$  bias. Inset diffraction patterns identify the phases.

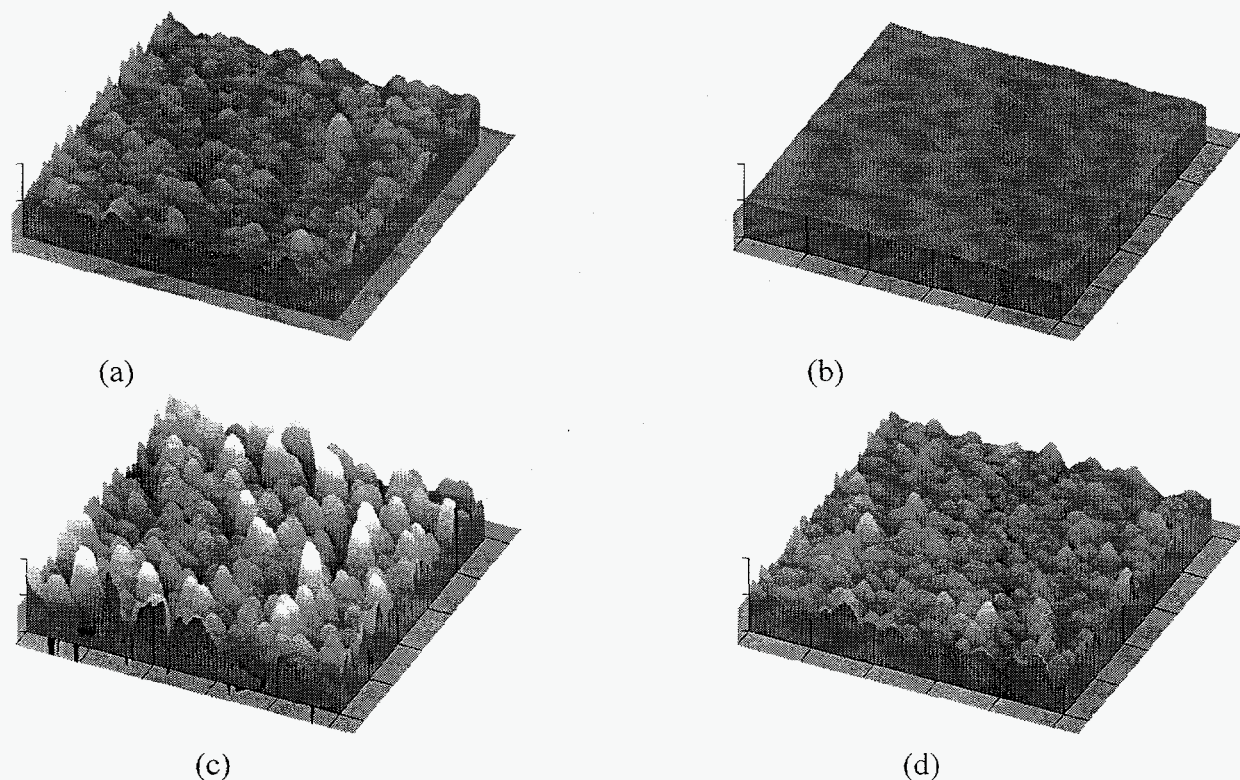


Fig. 2. AFM images over a  $1 \times 1\ \mu\text{m}^2$  area obtained from  $170\text{ nm}$  thick  $\text{Al}_2\text{O}_3$  films deposited at: (a)  $130^\circ\text{C}$  with no bias, (b)  $100^\circ\text{C}$  with an applied bias of  $-155\text{ V}$ , (c)  $400^\circ\text{C}$  with no bias, and (d)  $400^\circ\text{C}$  with a  $-150\text{ V}$  bias. The z-axis gray scale ranges from  $0 - 9\text{ nm}$  in all images.

an additional bias are still amorphous suggesting that both thermal and ion-induced mechanisms are required for *in-situ* formation of the crystalline phase. The type of microstructure and phase for these films is expected to affect the surface morphology in that amorphous films generally produce a smoother surface structure.

For comparison to the film microstructure, atomic force microscopy of the  $\text{Al}_2\text{O}_3$  films indicated that the rms surface roughness increased with substrate temperature and decreased with substrate bias. Figure 2 shows AFM images over a  $1\ \mu\text{m} \times 1\ \mu\text{m}$  area of 170 nm thick  $\text{Al}_2\text{O}_3$  films grown on a Si(100) substrate. The images on the right half of this figure show the effect of applying a bias during deposition, and the images in the lower half of this figure show the effect of a 400°C deposition temperature. These images were obtained using a silicon nitride microlever with a pyramidal tip having a nominal radius of curvature of 20 nm. It is well known that images from thin film samples may contain artifacts due to convolution of the tip shape with the true surface features when they have a radius of curvature less than the apex of the tip [9]. While our measured features are larger than the nominal tip radius, some tip artifacts may still be present in the images which would cause an error in an absolute surface roughness measurement. Nonetheless, the values we report here are valid for relative comparisons of surface morphology.

The sample deposited at 130°C with no bias (Fig. 2a) has a rms surface roughness of 0.8 nm while a film deposited at 100°C with a -155 V bias (Fig. 2b) has a rms value of 0.1 nm. Growth at 400°C without an applied bias yielded the largest rms value of 2.0 nm as shown in Fig. 2c. Finally, the sample deposited at 400°C with a -150 V bias (Fig. 2d) has a rms surface roughness of 0.8 nm. Therefore, the use of energetic ions (~180 eV for a bias of -150 V) during the growth of  $\text{Al}_2\text{O}_3$  forms a smoother film, whereas increasing the temperature to 400°C forms a rougher film. In fact, it should be noted that although the sample grown at 400°C without bias is amorphous, its surface has a greater roughness than the small-grain polycrystalline film grown *in situ* at 400°C with an applied bias. Thus variations in the substrate bias and temperature during deposition have a major influence in controlling the surface roughness.

## DISPERSION-STRENGTHENED $\text{AlO}_x$ FILMS

In this section we will examine the effect of deposition temperature and bias during deposition of Al films containing a dense dispersion of  $\gamma\text{-Al}_2\text{O}_3$  particles. These  $\text{AlO}_x$  films grown from an ECR oxygen plasma range in composition from 9 at.% O up to 26 at.% O. TEM results obtained from a sample with 26 at.% O grown at 127°C with no applied bias (Fig. 3a) revealed that the film microstructure consisted of fcc polycrystalline grains, ranging in size from 10 to 80 nm, with a fine dispersion of  $\gamma\text{-Al}_2\text{O}_3$  precipitates (not shown), ranging in size from 1 to 2 nm, within the Al grains. In contrast, Fig. 3b shows the rough microstructure produced when an  $\text{AlO}_x$  film (9 at.% O) is grown at 400°C with no applied bias. For this high temperature sample, Al grains up to 2  $\mu\text{m}$  in size were found on a layer of finer grains (down to 20 nm in size) and the smallest observed  $\gamma\text{-Al}_2\text{O}_3$  particles were  $\geq 4$  nm in size. This type of microstructure leads to a significantly softer film with a rougher surface as discussed below.

The AFM images (Fig. 4) clearly show that the rms surface roughness increased as both the deposition temperature and the applied sample bias increased.  $\text{AlO}_x$  films were deposited at 100°C without an applied bias and with an applied bias up to -300V. A film was also grown at 360°C without an applied bias. A comparison of Fig. 4a and Fig. 4b show that the rms surface roughness increased from 14.5 nm for the sample grown at 100°C without a bias to 23 nm for a

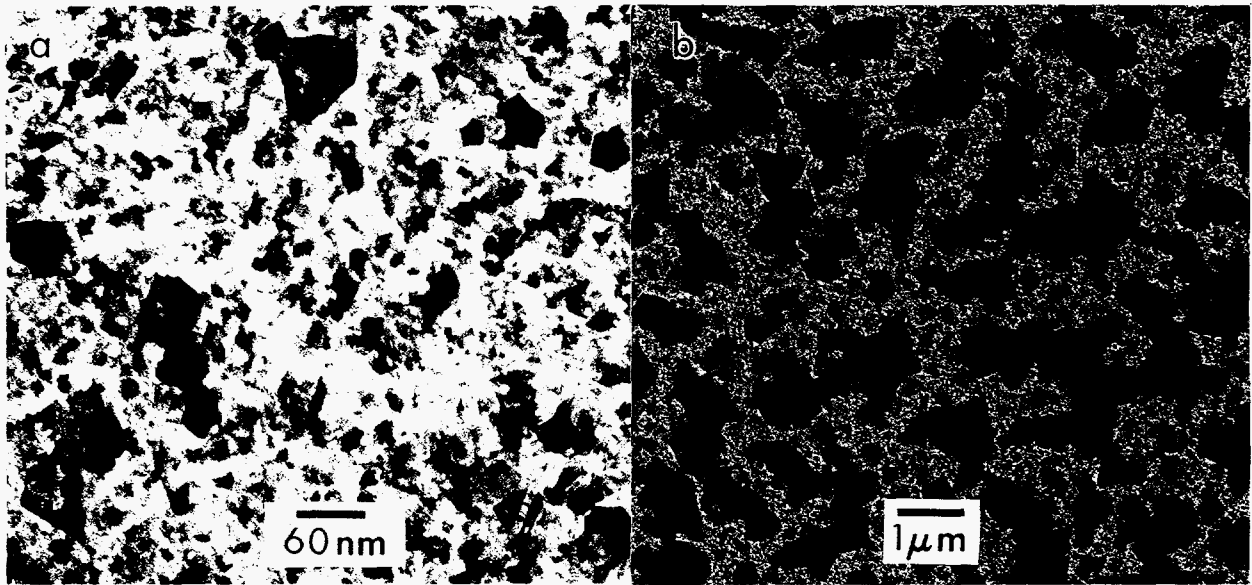


Fig. 3 Bright-field TEM images of a  $\text{AlO}_x$  films deposited onto  $\text{SiO}_x$ -coated TEM grids: (a) ECR Al (26 at.% O) deposited at  $127^\circ\text{C}$  with no applied bias showing polycrystalline Al grains ranging in size from 10 to 80 nm, and (b) ECR Al (9 at.% O) deposited at  $400^\circ\text{C}$  with no applied bias showing rough microstructure with Al grains up to 2  $\mu\text{m}$  in size.

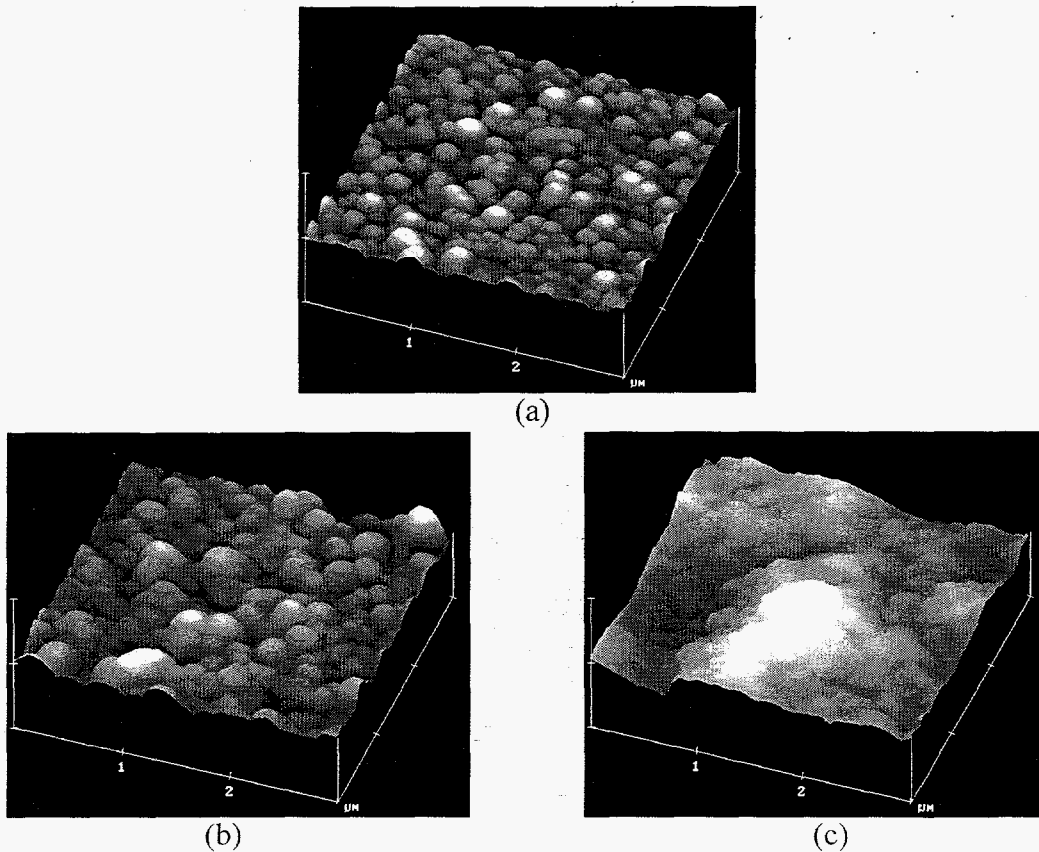


Fig. 4. AFM images over a  $3 \times 3 \mu\text{m}^2$  area obtained from  $\text{AlO}_x$  films deposited on Si (100) at (a)  $100^\circ\text{C}$  with no bias; rms roughness=14.5 nm; thickness 675 nm (b)  $100^\circ\text{C}$  with -300 V bias; rms roughness=23 nm; thickness 900 nm and (c)  $360^\circ\text{C}$  with no bias; rms roughness=105 nm; thickness 650 nm. The z-axis scale is from 0 to 600 nm in (a) and (b) and is 0 to 2000 nm in (c).

sample grown with a bias of -300 V. Further, Fig. 4c shows that an even rougher film (rms roughness=105 nm) is produced at a deposition temperature of 360°C. This sample is extremely rough and the large hillock surface morphology seen in the AFM image agrees well with the size and distribution of the large grains found in the planar TEM image of Fig. 3b. This increased surface roughness with deposition temperature is similar to that found for the stoichiometric oxide films, while the increased roughness with ion irradiation of the AlO<sub>x</sub> alloys is in contrast to that for the Al<sub>2</sub>O<sub>3</sub> films. Finally, the rms surface roughness of the AlO<sub>x</sub> alloys was found to be at least an order of magnitude greater than that for the oxide films shown in Fig. 2. These differences between the Al<sub>2</sub>O<sub>3</sub> and AlO<sub>x</sub> films may result from the large difference in the microstructures involved: amorphous to nanocrystalline Al<sub>2</sub>O<sub>3</sub> oxide films versus nanocrystalline to microcrystalline AlO<sub>x</sub> alloy films.

## CONCLUSIONS

Al<sub>2</sub>O<sub>3</sub> and AlO<sub>x</sub> layers were grown on Si(100) substrates with an applied bias up to -300 V over the temperature range of 100°C to 400°C. For the Al<sub>2</sub>O<sub>3</sub> films, the rms surface roughness increases with deposition temperature and decreases with applied bias; whereas for the AlO<sub>x</sub> films the rms surface roughness increases with both temperature and bias. This difference in behavior of the surface morphology is thought to be related to the different types of microstructure observed. The Al<sub>2</sub>O<sub>3</sub> films are amorphous or small grain nanocrystalline  $\gamma$ -Al<sub>2</sub>O<sub>3</sub>, while the AlO<sub>x</sub> films are larger grain polycrystalline Al containing a fine dispersion of  $\gamma$ -Al<sub>2</sub>O<sub>3</sub> precipitates. The rough surface morphology is expected to affect the tribological properties of these films, which are currently under investigation.

## ACKNOWLEDGMENTS and REFERENCES

The authors thank L. Griego, K. Minor, M. Moran, D.S. Walsh, and J.H. Burkhardt for technical assistance. This work was supported by the U.S. DOE Office of Basic Energy Sciences (Division of Materials Science and the Synthesis and Processing Center) under contracts: DE-FG02-90ER45417 (Maine) and DE-AC04-94AL85000 (Sandia).

- [1] D.M. Follstaedt, S.M. Myers, R.J. Boucier and M.T. Dugger, in Beam Processing of Advanced Materials (TMS, Metals Park, Ohio, 1992) p. 507.
- [2] D.M. Follstaedt, S.M. Myers and R.J. Boucier, Nucl. Instrum. and Meth. B **59/60**, 909 (1991).
- [3] R.J. Boucier, S.M. Myers and D.H. Polonis, Nucl. Instrum. and Meth. B **44**, 278 (1990).
- [4] R.J. Boucier, D.M. Follstaedt, S.M. Myers and D.H. Polonis, Mat. Res. Soc. Symp. Proc. **157**, 801 (1990).
- [5] R.J. Boucier, D.M. Follstaedt, M.T. Dugger and S.M. Myers, Nucl. Instrum. and Meth. B **59/60**, 905 (1991).
- [6] J.C. Barbour, D.M. Follstaedt and S.M. Myers, Nucl. Instrum. and Meth. B (in press).
- [7] J.C. Barbour, D.M. Follstaedt, J.A. Knapp, D.A. Marshall, S.M. Myers and R.J. Lad, Mat. Res. Soc. Symp. Proc. vol. **396** (in press).
- [8] J.A. Knapp, D.M. Follstaedt and S.M. Myers, J Appl. Phys. (in press).
- [9] K.L. Westra and D.J. Thomson, Thin Solid Films **257**, 15 (1995).

## DISCLAIMER

This report was prepared as an account of work sponsored by an agency of the United States Government. Neither the United States Government nor any agency thereof, nor any of their employees, makes any warranty, express or implied, or assumes any legal liability or responsibility for the accuracy, completeness, or usefulness of any information, apparatus, product, or process disclosed, or represents that its use would not infringe privately owned rights. Reference herein to any specific commercial product, process, or service by trade name, trademark, manufacturer, or otherwise does not necessarily constitute or imply its endorsement, recommendation, or favoring by the United States Government or any agency thereof. The views and opinions of authors expressed herein do not necessarily state or reflect those of the United States Government or any agency thereof.